

# Chapter 15

## Femoral Mechanics, Mobility, and Finite Element Analysis

Kelli H. Tamvada

**Abstract** Traditional analyses of long bone morphology, e.g., applying beam theory to imaged cross sections of bone or investigating diaphyseal curvature, examine the effect of skeletal variables on structural integrity separately, an approach that does not incorporate information on the entire bone. Finite element analysis allows exploration of the structural integrity of complete bones under specific loading conditions, providing a more detailed picture of precisely how morphological differences affect a bone's strength and patterns of stress and strain. Finite element analysis also allows complex variables such as differences in joint configurations between species to be modeled. Finite element models further allow the examination of how bones behave during simulations of particular activities, at various magnitudes of loading, and at different angles of excursion. Here I provide an overview of finite element analysis and examine how it contributes to studies of mobility using a case study of a human femur.

**Keywords** FEA • Femur • Biomechanics • Stress • Strain

Bony responses to mechanical loading, particularly the rate and frequency of loading, are well-documented (Goodship et al. 1979; Hert et al. 1969, 1971, 1972; Jones et al. 1977; Krolner and Toft 1963; Lanyon 1987; Lanyon and Bourn 1979; Lanyon et al. 1979, 1982; Nordstrom et al. 1996; Paul 1971; Ruff 2005; Ruff et al. 2006; Skerry 2000; Taylor et al. 1996; Tilton et al. 1980; Woo 1981). For this reason, bones are thought to be useful sources for understanding activity in populations or organisms whose activity cannot be directly observed. One aspect of activity is mobility, defined here as linear movement across the landscape (Carlson et al. 2007;

---

K.H. Tamvada (✉)

Department of Anthropology, University at Albany, State University of New York,  
1400 Washington Avenue, Albany, NY 12222, USA  
e-mail: [KTamvada@albany.edu](mailto:KTamvada@albany.edu)

Kelly 1995), which is often quantified as the ecological variable day range. Day range is the distance an animal or focal group typically travels in the pursuit of resources in the course of one day. Mobility patterns elucidate interesting aspects of culture in prehistoric societies such as subsistence strategies, hunting techniques, seasonal activity levels, home range size, resource availability, and other behavioral variables (Larsen 1987). In order to infer clues about mobility from bones, we must first identify which aspects of bony morphology are important in reconstructing mobility and why.

There are several characteristics of the human femur that are likely to be related to activity levels. These include neck-shaft angle (Trinkaus 1993), diaphyseal cross-sectional morphology and robusticity (i.e. relative biomechanical strength) (Cowgill, 2014; Ruff et al. 1993; Stock and Shaw 2007; Lieberman et al. 2003; Trinkaus and Ruff 1999; Trinkaus et al. 1999), and diaphyseal curvature (Bertram and Biewener 1988; Ruff 1995; Shackelford and Trinkaus 2002). Human infants are born with high neck-shaft angles, but as load-bearing begins, this angle decreases. Given the plastic nature of these traits in sub-adults, they may be indicative of activity levels during development (Cowgill 2010, 2014; Cowgill et al. 2010; Trinkaus 1993). Clearly, diaphyseal robusticity is related to activity levels in that frequent loading induces bony changes meant to reinforce the strength of the bone, usually through bone deposition on the periosteal surface, e.g., (Goodship et al. 1979; Hert et al. 1971, 1972; Lanyon and Baggott 1976; Lanyon et al. 1979). When elevated activity levels are a consequence of locomotion, then those activity levels may be associated with increased mobility. Aspects of shape, such as cross-sectional geometry and longitudinal curvature, serve to elevate and influence the predictability of stress transmission through the shaft (Bertram and Biewener 1988). Predictability of stress transmission may be an important adaptation to resisting eccentrically-directed loads (Bertram and Biewener 1988; Biewener et al. 1983). Thus, there are two means by which a bone may reinforce itself: size and shape, both of which must be considered when studying mobility. Each of these morphological traits is worthy of investigation, but the femur, like any other bone, is an integrated structure (Bertram and Biewener 1988; Currey 2002) rather than discrete characteristics (e.g., diaphyseal curvature, cross-sectional geometry) independently grouped together. Finite element models (FEMs) provide an advantage relative to two-dimensional analyses [such as applying beam analysis to variously imaged cross sections of bone (Ruff 1989)] in that they can potentially provide a more complete understanding of bone behavior under various, specified loading environments. For this reason, finite element analysis (FEA) has a promising role to play in mobility studies aimed at deciphering the effect of long bone morphology on bone behavior.

This method is particularly powerful in that, once a model is created and validated, an array of modeling experiments can be performed to test various questions regarding the modeled structure. In principle, such experiments are limited only by the accuracy of input data, such as geometry, material properties, or muscle force magnitudes and directions. Note, however, that FEA does not provide direct information about mobility patterns or ranging behavior. Rather, FEA provides a means of testing how well structures “perform” mechanically under specific loading

conditions that may simulate those experienced by an organism during particular behaviors. If these hypothesized conditions reflect those experimentally determined to be adaptive in organisms that, for example, range over long distances, then it is possible to test whether or not expressed morphologies of organisms confer a biomechanical advantage compared to alternative morphologies (e.g., structures of different shapes). For example, if it is hypothesized that a given bone is routinely loaded with high forces, or that it is loaded especially frequently, then one might hypothesize that the bone should exhibit a morphology that makes it structurally strong in the face of these loads. Alternatively, it might possess a shape that increases the predictability of its strain environment. In either case, these predictions are mechanical in nature, and importantly, they can be tested with FEA.

FEA is a remarkably powerful and flexible analytical tool. In principle, it should be possible to perform a series of experiments modeling the performance of a bony structure over the course of a given activity, e.g., a femur during running at different points of the gait cycle, or a humerus during the act of rowing a boat. Indeed, FEA can, in principle, be used to dynamically simulate complex behaviors. However, such applications would require detailed information about applied loads and kinematics that may not presently exist. It also would be interesting to examine the effect of bone remodeling, or changes in a structure's morphology, on its performance. In the case of remodeling, this could potentially be carried out by artificially altering the FEM so that periosteal deposition is simulated using Virtual Anthropology techniques (Weber and Bookstein 2011). Advances in the confluence of these two methods leave the field ripe for discovery (Weber et al. 2011).

The aim of this chapter is to give readers an overview of how FEA works, to illustrate potential research applications of FEMs in anthropology (focusing on mobility) with a human femur FEM test case, and to identify avenues of future research involving postcrania.

## 15.1 Finite Element Analysis: The Method

One purpose of FEA is to elucidate the manner or degree to which a structure responds to external loads. Key outputs of FEA include information about stress (force per unit area) and strain (change in length divided by original length) (Richmond et al. 2005) experienced by a loaded object. Two applications of FEA are of particular interest in this chapter. In the first application, biologically realistic models are created for use in experiments aimed at better understanding how the bone (or structure of interest) behaves under specific loading conditions. For this application, a well-validated model (discussed below) is of the utmost importance. The second application involves comparisons between similar structures, as may occur when comparing different fossil taxa. In other words, how do different skeletal designs compare mechanically to one another? For example, how do differences in femoral shape and size between the Neanderthal and modern human lower limb affect each system's ability to withstand loads associated with walking? Since

muscle force data, and to some degree, body mass data, are unknowable for extinct taxa, this application is better employed when investigating relative abilities of structures to resist loads.

There are four main steps involved in FEA: model creation, model solving, and validation followed by interpretation. The first step, model creation, is often the most time-consuming process. During model creation, the investigator makes decisions regarding the geometric design of the structure of interest, boundary conditions, material properties, and the loads that will be applied to the model. Once a model is created, it is solved by computer hardware and software capable of performing a vast number of mathematical equations that result in stress, strain, and displacement calculations for the entire structure. Afterwards, the really interesting questions can be asked. For example, are the results realistic, and what do they mean in a biological context?

Finite element models of skeletal structures are typically created from serial computed tomography (CT) scans so that both external and internal geometry can be modeled. Tessellated surface models, which are composed of hundreds of thousands of geometrically simple surfaces (such as triangles) arranged in a mosaic pattern and enclosing volumes representing bone, are generated using medical imaging software in a multi-step process. These software programs typically require the use of a combination of manual and automatic thresholding techniques to separate trabecular bone from cortical bone, and bone from air. This procedure can be quite time consuming, but long bones, particularly the diaphysis, that are key components of mobility studies, have relatively simple geometries and thus are less difficult to model than skeletal structures like crania. Once separate volumes of bone are created, they are divided into a large, but finite number of elements of a simple shape, joined together at vertices called nodes. These simple shapes collectively create the mesh that comprises a model. Depending on the software being used, these shapes may be tetrahedra or “bricks” with a varying number of nodes and sides. As the number of nodes and/or elements increases, the accuracy of the model should increase, but a trade-off is incurred since more computational power is needed to solve the model (Richmond et al. 2005).

Following creation of a FEM, it must be assigned material properties. In the case of a femur, the relevant material is bone. Key properties include the elastic modulus and Poisson’s ratio. The elastic modulus,  $E$ , describes how much strain a structure will experience in response to a given stress when the object is loaded axially. More specifically, it represents the slope of the linear (elastic) portion of the stress–strain curve for a given material. This describes the stiffness of the object during tension or compression. Poisson’s ratio ( $\nu$ =lateral strain/axial strain) describes how much the sides of an object will contract or expand laterally during tensile or compressive axial loads, respectively. If a material is isotropic, then its material properties are the same in all directions at any given point, and thus the elastic modulus and Poisson’s ratio are the only two properties that need to be specified. Most FEA studies assume that cortical bone is isotropic, but this is typically not the case in life. Rather, bone tends to range between being roughly transversely isotropic (i.e., material properties in the axial direction of a long bone may differ from those in the cross section

of the bone) to being orthotropic (material properties vary in each of three orthogonal directions). Moreover, most FEA studies assume that the material properties of cortical bone are spatially homogenous (i.e., they are the same in all regions of the bone), when in fact those properties may be heterogeneously distributed [i.e., they may vary from region to region (Bozanich et al. 2009; Wang et al. 2006)]. Finally, cortical and trabecular bone have different elastic moduli; cortical bone is much stiffer than trabecular bone (Currey 2002).

Constraints and applied forces are referred to as boundary conditions. It is necessary to constrain the model from moving in at least some fashion, although it is also important not to overly constrain it as that may result in unrealistic stresses and/or strains throughout the model (Richmond et al. 2005). The application of constraints ensures that models resist translational or rotational movement; it anchors them in three-dimensional space and ensures that the applied forces will cause deformations in the model. Constraints are typically chosen in locations imitating biological constraints, such as ligaments, or contact between bones. For instance, when modeling a femur, one might choose to apply constraints at the fovea capitis on the femoral head and on the distal-most surface of the epiphyses to simulate contact with the tibial plateau. Because the selected nodes are not allowed to move, strain will be concentrated at and around those locations, possibly producing unrealistic local strains. Therefore, if possible, it is best to analyze strain at locations away from the constraints so as not to bias the results of the experiment.

Muscle forces can be applied to the model as vectors running from the origin of a muscle towards its insertion. Muscles with multiple compartments that may not all act simultaneously are best modeled with multiple origins, or as separate muscles. Ideally, surface models of bones articulating with the bone of interest will be positioned such that they can serve as origin and insertion points for the muscles. For instance, surface models of the pelvis, tibia, and fibula may be necessary to apply muscle forces to a femur FEM during simulation of bipedal walking insofar as many muscles active during walking either arise from or insert on one of these surrounding bones.

Once a model has been created, volumes have been assigned material properties, and boundary conditions have been applied, it is possible to solve the model and interpret results. Computer software solves the model by calculating nodal displacements due to applied forces, and the stresses and strains corresponding to these nodal displacements (Zienkiewicz et al. 2005).

Once a model has been solved, there is not yet reason to be confident that the model accurately depicts what happens in a real biological system. In order to know this, the investigator must validate the model. Preferably, this would mean comparing strain data obtained from the FEM of a bone to strain data obtained from *in vivo* measurements by strain gages affixed to the same bone during the same loading scenario as was applied to the FE model of the bone. However, this is not always possible due to both practical and ethical reasons (in the case of humans and animals, respectively) as the procedure is highly surgically invasive, and is not even the norm, especially for experiments focusing on human subjects. In cases where *in vivo* strain gage measurements are impossible to obtain, *in vitro* cadaveric experiments are a reasonable alternative. However, *in vivo* and *in vitro* validation

experiments measure different things. Generally speaking, in vitro bone strain experiments entail the application of forces that only coarsely approximate those used in actual behaviors. However, an advantage of such studies is that it is generally relatively straightforward to simulate those loads (as well as constraints) in FEA. Thus, in vitro validation is most useful in assessing the validity of the geometry and material properties of a bony structure. In contrast, in vivo validation experiments examine the degree to which all of the assumptions incorporated into the simulation of a behavior (e.g., geometry, loads, constraints, material properties) are collectively valid. In a perfect scenario, FEMs would be validated using both in vivo and in vitro data, although this is not typically done. Regardless, a well-validated model is essential if the purpose is to realistically depict the performance of a structure in a biological context. Once it is reasonably certain that the FEM behaves in a biologically realistic manner, loads or other input variables can be changed to reflect those obtained from in vivo experiments, and interpretation of the results may proceed with a level of confidence equal to the rigor of the validation test.

Examination of the patterns of stress or strain due to specific loads allows an investigator to identify weak points in the structure, the overall pattern of deformation, or how each set of loading conditions affects the behavior of the model. Applying the same loads to different models shows how size *and* shape differences in the structures affect each structure's ability to resist loads. However, when comparing bones of different morphology, an investigator may want to know what effect shape alone has on stress and strain. By scaling magnitudes of forces applied to a FEM by the volume of a model raised to the  $2/3$  power, one can remove size as a factor in FEA experiments and simply compare the effects of scale-free shape differences (Dumont et al., 2009).

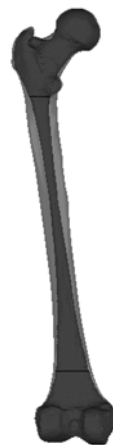
## 15.2 Finite Element Analysis of a Human Femur

### 15.2.1 Model Creation

Serial computed tomography (CT) scans of a modern human femur were first imported as TIFF files and processed in the computer software program Mimics v13 (Materialise, Ann Arbor, MI, USA), in which surface meshes composed of triangles were created. An automatic thresholding algorithm was used to separate bone from empty space. Then, through manual slice-by-slice segmentation, three separate surfaces were generated representing the outer layer of cortical bone, and two volumes of trabecular bone, one each in the proximal and distal ends of the bone. The medullary cavity was modeled as an empty space (Fig. 15.1).

These surfaces were exported into the surface editing program Geomagic Studio v12 (Research Triangle Park, NC, USA) as binary STL files. In Geomagic Studio, surfaces were rid of imperfections such as holes, overlapping triangles, spikes, and other abnormalities or distortions created during the manual segmentation process.

**Fig. 15.1** The human FEM displayed transparently in the surface editing program Geomagic Studio, with solid black lines marking divisions between proximal and distal volumes of trabecular bone and the central medullary cavity



Once the geometry was judged to be clean, surfaces were re-imported into Mimics where they were once again meshed to check for overlapping triangles. If no intersections were found, surfaces were volume meshed to create watertight solid volumes composed of thousands of tiny tetrahedral elements connected by nodes, rather than simple surfaces. The end result of this process was four mutually exclusive volumes: outer cortical bone, inner medullary cavity, proximal and distal trabecular bone.

Each volume was imported into the Strand7 Finite Element Analysis Software System (Strand7 Pty Ltd, Sydney, NSW) as a NASTRAN file. Strand7 allows the application of various material properties, constraints, and force loads. In this model, the medullary cavity volume was deleted, leaving an empty space inside the volume of cortical bone, which separated each trabecular bone volume (Fig. 15.1). Volumes were assigned isotropic material properties. Cortical bone was given an elastic modulus ( $E$ ) of 20 gigapascals (GPa), and a Poisson's ratio ( $\nu$ ) of 0.3 (Currey and Butler 1975). Trabecular bone was modeled as a solid rather than as individual trabeculae due to the prohibitively time-consuming nature of the task. Trabecular bone was assigned  $E=749$  megapascals (MPa) and  $\nu=0.3$  (Kaneko et al. 2004; Strait et al. 2005).

### 15.2.2 Constraints

Constraints were applied at seven locations on the femur (Fig. 15.2). One node within the fovea capitis was constrained from anteroposterior (AP) and mediolateral (ML) movement to simulate ligamentum teres. One node on the inferior most surface of each femoral condyle was constrained from moving in the vertical direction. This simulates contact between the femur and the tibia. One node on the inner surface of each condyle within the intercondylar groove was constrained from moving

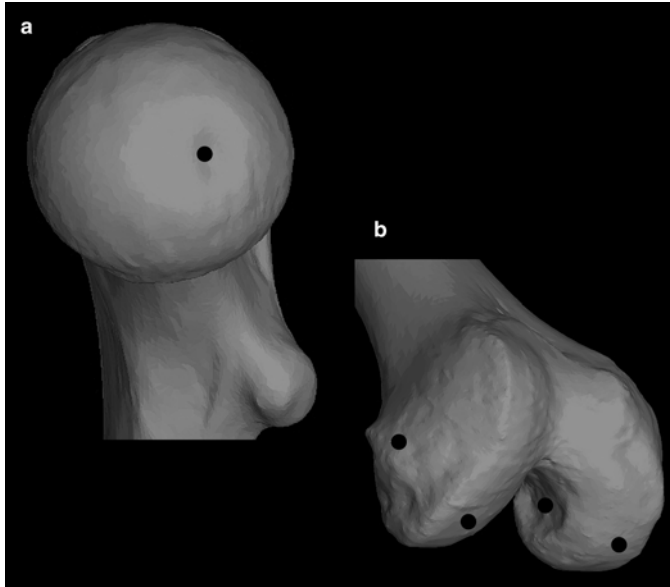


**Fig. 15.2** Constraints, marked with black dots, were applied to one location on the femoral head (a) and six nodes on the distal end (b) of the FEM. Constraints represent the effect of contact with ligamentum teres, the tibial plateau, the cruciate ligaments, and collateral ligaments. Note that constraints representing the medial collateral ligament and the lateral attachment of the cruciate ligaments are not shown, but mirror their counterparts

in the AP direction, simulating the effect of the cruciate ligaments. Finally, one node was constrained from moving in the ML direction on the lateral surfaces of each epicondyle, corresponding to the collateral ligaments. It is important not to over-constrain the FEM, as would be the case if a region of nodes corresponding to the cross-sectional area of each ligament was constrained, since this can have an adverse effect on results (Haut Donahue et al. 2002).

### 15.2.3 Validation

This FEM was validated by replicating a cadaveric experiment conducted by Huiskes (1982). In that experiment, an embalmed human femur, dissected free of all soft tissue, was secured in a laboratory setting, and loaded with strain gages at seven horizontal levels along the diaphysis (Fig. 15.3). At each of these horizontal levels, seven strain gages were applied to the circumference of the diaphysis to measure maximum and minimum principal stress. Ten thousand Newton millimeters (Nmm) of torque were applied to the femoral head; the resulting principal stresses were measured at 49 locations on the diaphysis of the femur. In order to recreate the loading regime of the cadaveric femur used by Huiskes (1982) for the femur FEM, it



**Fig. 15.3** Location of the seven horizontal levels around the femoral diaphysis indicating areas where strain gages were affixed and stress was measured [modified from Huiskes (1982)]. The first location at each level begins at the dotted vertical line along the posterior diaphysis and subsequent points of stress are measured at even intervals proceeding medially as indicated by the arrow and letter “s”

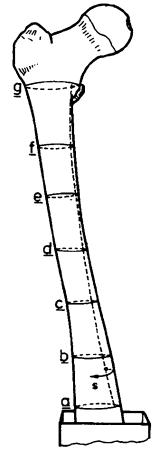
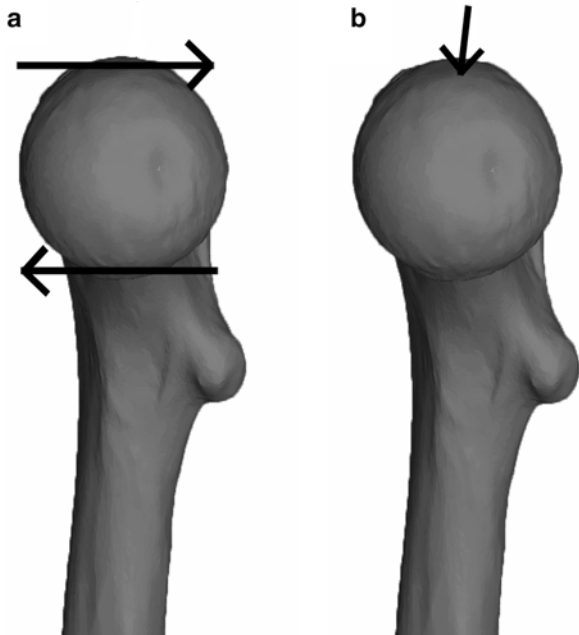


**Fig. 15.4** Medial view of forces applied to the femoral head in the validation study (a) and simulation of loading during gait (b). In the validation study (a), 227.27 N were directed anteriorly and posteriorly as indicated by the solid black arrows inferiorly and superiorly, respectively. In the simulation of loading during gait, a resultant force of 1,951 N was applied to the superior portion of the femoral head (b). Solid black arrow indicates direction of applied force



was determined that the force couple producing 10,000 Nmm torque in the human cadaveric femur was 454.54 N for a femoral head with a radius of 22 millimeters (mm), as in the FEM. In order to create a torque, two forces (one each directed posteriorly and anteriorly) were applied to the femoral head. So  $(10,000 \text{ Nmm} / (22 \text{ mm})) / 2 = 227.27 \text{ N}$ . Therefore a 227.27 N force directed posteriorly was applied to the superior portion of the femoral head, and a 227.27 N force directed anteriorly was applied to the inferior surface of the femoral head (Fig. 15.4a).

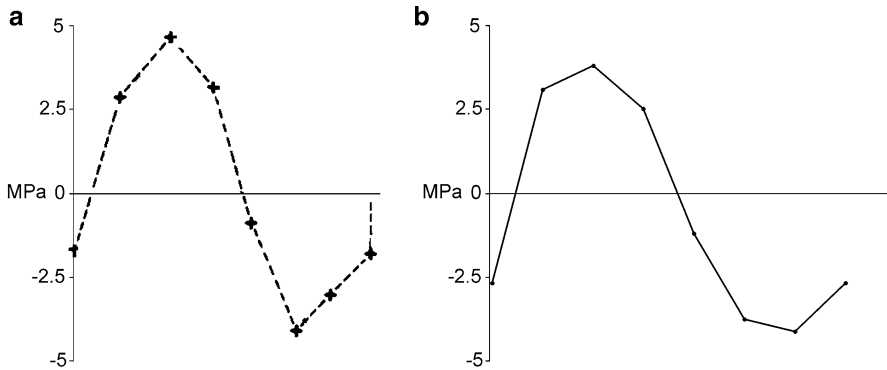


**Fig. 15.5** Stress, recorded at seven locations along the midshaft circumference by strain gages affixed to a cadaveric human femur [modified from Huijkes (1982)] (a), is compared to stress measured along the midshaft diaphysis on the FEM (b). Location corresponds to level “d” in Fig. 15.3

Once the model was solved in Strand7, maximum and minimum principal stresses were measured at approximately the same locations as on the cadaveric femur (Fig. 15.3); the data show a close correspondence in both pattern and magnitude (Fig. 15.5). When subjected to a posterior bending moment, the femur experiences tension along the anterior portion of the diaphysis, and compression posteriorly, as does the femur FEM.

### 15.2.4 Simulation of Loading Conditions During Gait

Once the femur FEM is satisfactorily validated, it is used to simulate a more biologically interesting loading condition, namely the instant of peak acetabular force during push-off, directly prior to toe-off. In principle, one could model the femur dynamically as it is loaded throughout an entire gait cycle, but this introduces considerable complexity into the modeling procedure. As an alternative, the femur was modeled statically using the forces corresponding to the instant of peak acetabular force (although, there are many informative events within the gait cycle, such as at peak vertical substrate reaction force and peak acetabular force at heel strike). Pedersen et al. (1997) used a combination of kinematic and kinetic methods along with an optimization procedure to calculate acetabular force magnitude and direction, as well as the magnitudes of the forces of 22 hip and thigh muscles at 32 intervals during the gait cycle. At push-off, acetabular force was calculated to equal 314.8 % body weight, and was divided into three component directions (vertical, ML, and AP) with a resultant force of 1951 Newtons (N) (Table 15.1). These forces were applied to a rectangular selection of bricks on the femoral head of the model (Fig. 15.4b). Of the 22 muscles monitored by Pedersen et al. (1997), ten were active during the gait event (Table 15.1). Muscle forces were applied using the

**Table 15.1** Forces applied to the human FEM

<i>Axial force (N)</i>	
Vertical	1,859
Mediolateral	555
Anteroposterior	214
<i>Muscle forces (N)</i>	
Gluteus maximus	420
Gluteus medius	286
Gluteus minimus	124
Biceps femoris	256
Psoas major	71
Iliacus	91
Gemellus superior	3
Gemellus inferior	7
Obturator internus	40
Piriformis	98

*Source:* Pedersen et al. (1997)

tangential-plus-normal loading procedure of Boneload (Grosse et al. 2007), a software package that interfaces with Strand7 allowing the modeling of complex muscle vectors that wrap around the surface of a model. Surface models of a pelvis and tibia belonging to the same individual as the femur from which the model was built were used to determine muscle attachment sites. Muscle forces were applied as the femur was in a slightly extended position relative to the pelvis, as would occur during push-off (Fig. 15.6). Some muscles, such as the adductors, with a linearly large attachment site were divided and measured in multiple components by Pedersen et al. (1997). We followed their procedure for dividing those muscles, and otherwise origin/attachment sites were directed from/to the center of the attachment site. Loads were applied to regions on the femur and were directed outward, either to the origin or insertion site, depending on the muscle. For example, gluteus medius originates from a large area on the ilium, and although it is a large muscle, it has a small insertion area on the greater trochanter of the femur. The entire insertion region received a load of 286 N (Table 15.1) divided evenly over its surface area and directed towards the center of origin on the ilium.

### 15.2.5 Results

Results show that a band of tension, as evidenced by maximum principal stress, begins on the lateral aspect of the greater trochanter and continues down and across the anterior diaphysis, ending on the anteromedial metaphysis (Fig. 15.7a). Similarly, but conversely, a band of compression, shown by minimum principal stress, originates on the posterior femoral head and continues down the femoral neck to the posterior diaphysis where it ends on the posterolateral metaphysis (Fig. 15.7b). Von Mises stress is most closely related to bone failure (Keyak and

**Fig. 15.6** The femur FEM is articulated with surface models of the pelvis and tibia in the approximate positioning of the lower limb during the instant of the gait cycle directly prior to toe-off. These positions were used to direct muscle vectors in the gait simulation experiment

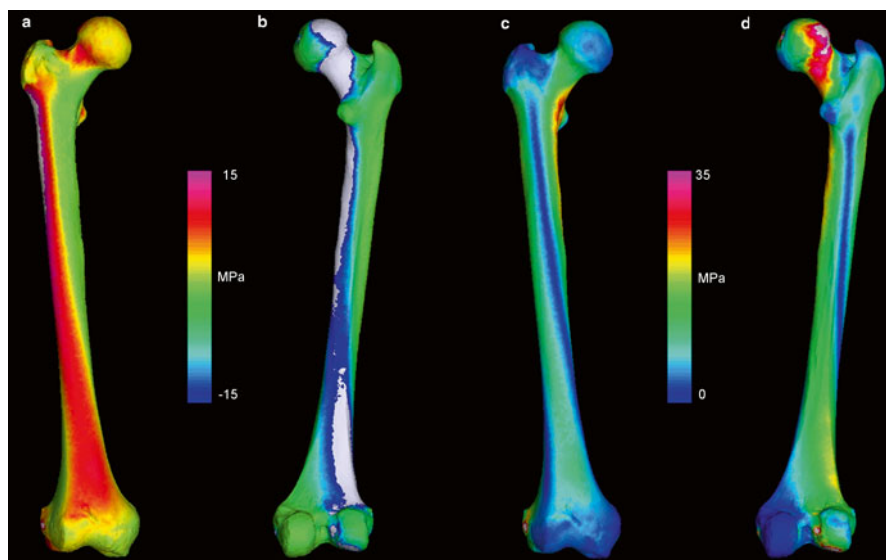


**Fig. 15.7** Maximum principal stress (a) displayed on an anterior view of the FEM shows where the model experiences highest tensile stresses. Minimum principal stress (b) is shown on a posterior view of the human FEM. The posterior diaphysis and femoral neck experience compression in this loading environment. Von Mises stress patterns follow those of maximum and minimum principal stress, anteriorly (c) and posteriorly (d), respectively, but are highest on the posterior side where the model experiences compression. Units are in megapascals

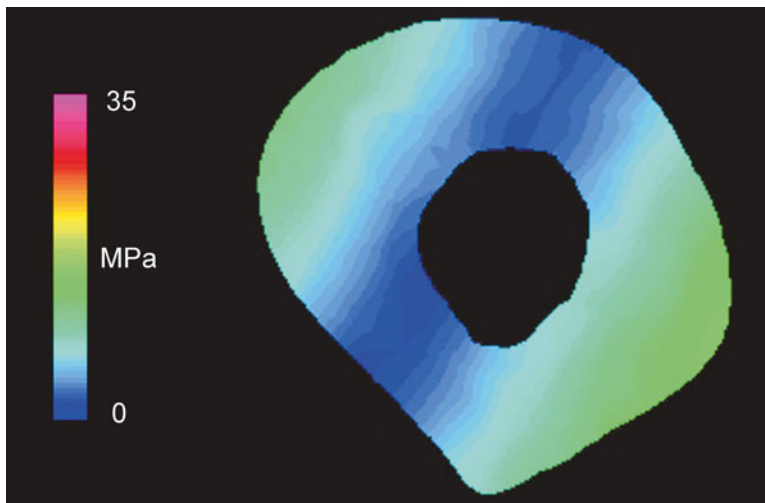


**Fig. 15.8** Midshaft diaphyseal cross section showing von Mises stress. The area experiencing the least amount of stress is indicated in *blue*, showing the axis about which the bone bends

Rossi 2000); patterns of von Mises stress follow maximum and minimum principal stresses on the anterior (Fig. 15.7c) and posterior (Fig. 15.7d) diaphysis, respectively, but are higher posteriorly where the model experiences compression. Regions of highest von Mises stress produced by these loads are found on the femoral neck, posterolateral distal metaphysis, posterior diaphyseal midshaft, and lateral proximal diaphysis (in order of highest to lowest stress).

### 15.2.6 Implications

Two key biomechanical insights provided by this FEA are relevant to interpretations of mobility. First, as evidenced by analyses of diaphyseal cross sections, midshaft bending is primarily ML rather than AP in orientation (Fig. 15.8). If interpretations about mobility depend on interpretations of femoral strength, then it follows that the key measure of strength is ML bending strength. Although modern human femora are deeper anteroposteriorly than they are mediolaterally (Trinkaus and Ruff 1999), it nonetheless appears that ML strength is the key variable limiting bone failure, at least during normal walking on a level surface. Secondly, cross-sectional analyses of strength typically rely on assumptions about the location of the neutral axis and the bending direction of a bone; this study corroborates other work suggesting that such assumptions may not strictly apply (Lieberman et al. 2004).

### 15.3 Future Directions

Implications of the FEA described above are, at present, limited, but they point the way towards future research that has the potential to be more informative about mobility. First, it is possible in principle to simulate other loading conditions. For example, using the acetabular and muscle force data gathered from Pedersen et al. (1997), it should be possible to model any event during a gait cycle corresponding to walking on level ground. Moreover, if one could gather adequate kinematic and kinetic data, one could potentially simulate walking on sloped or uneven terrain as well as the effect of changing directions during locomotion, topics of considerable interest in mobility studies (Carlson, 2014; Carlson and Judex 2007; Daley and Biewener 2006; Demes et al. 2001, 2006). One could also model running on a variety of terrains, or leaping and landing in order to investigate the effect of substrate use on stress transmission (Demes et al. 1995). One could also model stumbling, which might represent a load case more likely to cause injury (and threaten bone integrity) than habitual running or walking (Daley and Biewener 2006). Specific hypotheses exist regarding trade-offs between high and low leg retraction velocities relating to injury and stumbling risk when running over uneven terrain (Daley and Usherwood 2010), hypotheses that might be testable using FEA. In addition, one could simulate traumatic blows. One might potentially find that femora that are strong under one loading regime might be weak under another, and this might lead researchers to a more nuanced understanding of the selection forces that may have influenced the evolution of femoral form. Furthermore, application of FEA is not limited to femora. Other postcranial elements that are the subject of studies of mobility include the fibula (Sparacello et al., 2014), humerus (Marchi et al. 2006), tibia (Demes et al. 2001), or multiple elements considered together (Sparacello and Marchi 2008; Stock 2006).

Major insights about mobility and femoral functional anatomy are likely to emerge through comparative biomechanics. For example, it has been hypothesized that Neanderthals ranged more widely than modern humans because metric analysis suggests that their femora were very strong. Comparisons of finite element models of modern human and Neanderthal femora could test this hypothesis with respect to specific loading conditions, and quantify the mechanical differences between them.

### 15.4 Summary

There are many hypotheses about activity (broadly) and mobility (in particular) that make predictions regarding long bone biomechanics. We want to understand the consequences of different activity levels and patterns of mobility on skeletal morphology, whether to reconstruct prehistoric lifeways, ranging behavior, or even to understand modern orthopedics. FEA is a versatile tool that allows the modeling of

bone behavior under various loading environments. The results of FEA provide insights into how bones perform mechanically as whole structures. Although FEA is a time-intensive process, the rewards are potentially great as the versatility of FEMs allows many hypotheses to be tested in an integrative manner.

**Acknowledgements** This study was supported by NSF BCS 1060835 and NSF BCS 0725126. I am especially grateful to Dr. David Strait for his helpful reviews and comments.

## References

- Bertram JEA, Biewener AA (1988) Bone curvature: sacrificing strength for load predictability. *J Theor Biol* 131:75–92
- Biewener AA, Thomason J, Goodship AE, Lanyon LE (1983) Bone stress in the horse forelimb during locomotion at different gaits: a comparison of two experimental methods. *J Biomech* 16:565–576
- Bozanic J, Byron CD, Chalk J, Grosse IR, Lucas PW, Richmond BG, Ross CF, Slice DE, Smith AL, Spencer MA, et al. Density and material orientation in ape mandibular cortical bone; 2009 April 1–4, Miami.
- Carlson KJ (2014) Linearity in the real world—an experimental assessment of non-linearity in terrestrial locomotion. In: Carlson KJ, Marchi D (eds) *Reconstructing mobility: environmental, behavioral, and morphological determinants*. Springer, New York
- Carlson KJ, Grine FE, Pearson OM (2007) Robusticity and sexual dimorphism in the postcranium of modern hunter-gatherers from Australia. *Am J Phys Anthropol* 134:9–23
- Carlson KJ, Judex S (2007) Increased non-linear locomotion alters diaphyseal bone shape. *J Exp Biol* 210:3117–3125
- Cowgill LW (2010) The ontogeny of Holocene and Late Pleistocene human postcranial strength. *Am J Phys Anthropol* 141:16–37
- Cowgill LW (2014) Femoral diaphyseal shape and mobility: an ontogenetic perspective. In: Carlson KJ, Marchi D (eds) *Reconstructing mobility: environmental, behavioral, and morphological determinants*. Springer, New York
- Cowgill LW, Warrener A, Pontzer H, Ocobock C (2010) Waddling and toddling: the biomechanical effects of an immature gait. *Am J Phys Anthropol* 143:52–61
- Currey J (2002) *Bones: structure and mechanics*. Princeton University Press, Princeton
- Currey JD, Butler G (1975) The mechanical properties of bone tissue in children. *J Bone Joint Surg* 57-A:810–814
- Daley MA, Biewener AA (2006) Running over rough terrain reveals limb control for intrinsic stability. *Proc Natl Acad Sci U S A* 103(2):15681–15686
- Daley MA, Usherwood JR (2010) Two explanations for the compliant running paradox: reduced work of bouncing viscera and increased stability in uneven terrain. *Biol Lett* 6:418–421
- Demes B, Carlson KJ, Franz TM (2006) Cutting corners: the dynamics of turning behaviors in two primate species. *J Exp Biol* 209:927–937
- Demes B, Jungers WL, Gross TS, Fleagle JG (1995) Kinetics of leaping primates: influence of substrate orientation and compliance. *Am J Phys Anthropol* 96(4):419–429
- Demes B, Qin Y-X, Stern JT Jr, Larson SG, Rubin CT (2001) Patterns of strain in the macaque tibia during functional activity. *Am J Phys Anthropol* 116(4):257–265
- Dumont E, Grosse I, Slater G (2009) Requirements for comparing the performance of finite element models of biological structures. *J Theor Biol* 256:96–103
- Goodship AE, Lanyon LE, MacFie H (1979) Functional adaptation of bone to increased stress. *J Bone Joint Surg* 61-A:539–546

- Grosse IR, Dumont ER, Coletta C, Tolleson A (2007) Techniques for modeling muscle-induced forces in finite element models of skeletal structures. *Anat Rec* 290(9):1069–1088
- Haut Donahue TL, Hull ML, Rashid MM, Jacobs CR (2002) A finite element model of the human knee joint for the study of tibio-femoral contact. *J Biomech Eng* 124:273–280
- Hert J, Liskova M, Landa J (1971) Reaction of bone to mechanical stimuli. Part I. Continuous and intermittent loading of tibia in rabbit. *Folia Morphol* 19:290–300
- Hert J, Liskova M, Landgrot B (1969) Influence of the long-term continuous bending on the bone. An experimental study on the tibia of the rabbit. *Folia Morphol* 17:389–399
- Hert J, Pribylova E, Liskova M (1972) Reaction of bone to mechanical stimuli. Part 3. Microstructure of compact bone of rabbit tibia after intermittent loading. *Acta Anat* 82:218–230
- Huiskes R (1982) On the modelling of long bones in structural analyses. *J Biomech* 15(1):65–69
- Jones HH, Priest JD, Hayes WC, Tichenor CC, Nagel DA (1977) Humeral hypertrophy in response to exercise. *J Bone Joint Surg* 59A:204–208
- Kaneko TS, Bell JS, Pejcić MR, Tehranzadeh J, Keyak JH (2004) Mechanical properties, density, and quantitative CT scan data of trabecular bone with and without metastases. *J Biomech* 37:523–530
- Kelly RL (1995) *The foraging spectrum-diversity in hunter-gatherer lifeways*. Smithsonian Institution Press, Washington
- Keyak JH, Rossi SA (2000) Prediction of femoral fracture load using finite element models: An examination of stress- and strain-based failure models. *J Biomech* 33:209–214
- Krolner B, Toft B (1963) Vertebral bone loss, an unheeded side effect of therapeutic bed rest. *Clin Sci* 64:537–540
- Lanyon LE (1987) Functional strain in bone tissue as an objective, and controlling stimulus for adaptive bone remodelling. *J Biomech* 20(11/12):1083–1093
- Lanyon LE, Baggott DG (1976) Mechanical function as an influence on the structure and form of bone. *J Bone Joint Surg* 58-B(4):436–443
- Lanyon LE, Bourm S (1979) The influence of mechanical function on the development and remodeling of the tibia: an experimental study in sheep. *J Bone Joint Surg* 61:263–273
- Lanyon LE, Goodship AE, Pye CJ, MacFie H (1982) Mechanically adaptive bone remodeling. *J Biomech* 15:141–154
- Lanyon LE, Magee PT, Baggott DG (1979) The relationship of functional stress and strain to the processes of bone remodeling. An experimental study on the sheep radius. *J Biomech* 12:593–600
- Larsen CS (1987) Bioarchaeological interpretations of subsistence economy and behavior from human skeletal remains. *Adv Archaeol Method Theory* 10:339–445
- Lieberman DE, Pearson OM, Polk JD, Demes B, Crompton AW (2003) Optimization of bone growth and remodeling in response to loading in tapered mammalian limbs. *J Exp Biol* 206:3125–3138
- Lieberman DE, Polk JD, Demes B (2004) Predicting long bone loading from cross-sectional geometry. *Am J Phys Anthropol* 123:156–171
- Marchi D, Sparacello VS, Holt BM, Formicola V (2006) Biomechanical approach to the reconstruction of activity patterns in Neolithic Western Liguria, Italy. *Am J Phys Anthropol* 131:447–455
- Nordstrom P, Thorsen K, Bergstrom E, Lorentzon R (1996) High bone mass and altered relationships between bone mass, muscle strength, and body constitution in adolescent boys on a high-level of physical-activity. *Bone* 19:189–195
- Paul JP (1971) Load actions on the human femur in walking and some resultant stresses. *Exp Mech* 11:121–125
- Pedersen DR, Brand RA, Davy DT (1997) Pelvic muscle and acetabular contact forces during gait. *J Biomech* 30(9):959–965
- Richmond BG, Wright BW, Grosse I, Dechow PC, Ross CF, Spencer MA, Strait DS (2005) Finite element analysis in functional morphology. *Anat Rec A Discov Mol Cell Evol Biol* 283A:259–274



- Ruff C (1995) Biomechanics of the hip and birth in early *Homo*. *Am J Phys Anthropol* 98: 527–574
- Ruff C (2005) Mechanical Determinants of Bone Form: Insights from Skeletal Remains. *Muculoskelet Neutonal Interact* 5(3):202–212
- Ruff C, Holt B, Trinkaus E (2006) Who's afraid of the big bad Wolff?: "Wolff's Law" and bone functional adaptation. *Am J Phys Anthropol* 129:484–498
- Ruff CB (1989) New approaches to structural evolution of limb bones in primates. *Folia Primatol* 53:142–159
- Ruff CB, Trinkaus E, Walker A, Larsen CS (1993) Postcranial robusticity in *Homo*. I: Temporal trends and mechanical interpretation. *Am J Phys Anthropol* 91:21–53
- Shackelford LL, Trinkaus E (2002) Late Pleistocene human femoral diaphyseal curvature. *Am J Phys Anthropol* 118:359–370
- Skerry TM (2000) Biomechanical influences on skeletal growth and development. In: O'Higgins P, Cohn MJ (eds) *Development growth and evolution: implications for the study of the hominid skeleton*. Academic, San Diego, pp 29–39
- Sparacello V, Marchi D (2008) Mobility and subsistence economy: a diachronic comparison between two groups settled in the same geographical area (Liguria, Italy). *Am J Phys Anthropol* 136:485–495
- Sparacello V, Marchi D, Shaw C (2014) The importance of considering fibular robusticity when inferring the mobility patterns of past populations. In: Carlson KJ, Marchi D (eds) *Reconstructing mobility: environmental, behavioral, and morphological determinants*. Springer, New York
- Stock J (2006) Hunter-gatherer postcranial robusticity relative to patterns of mobility, climatic adaptation, and selection for tissue economy. *Am J Phys Anthropol* 131(2):194–204
- Stock J, Shaw C (2007) Which measures of diaphyseal robusticity are robust? A comparison of external methods of quantifying the strength of long bone diaphyses to cross-sectional geometric properties. *Am J Phys Anthropol* 134:412–423
- Strait DS, Qiang Q, Dechow PC, Ross CF, Richmond BG, Spencer MA, Patel BA (2005) Modeling elastic properties in finite-element analysis: How much precision is needed to produce an accurate model? *Anat Rec A Discov Mol Cell Evol Biol* 283A(2):275–287
- Taylor ME, Tanner KE, Freeman MAR, Yettam AL (1996) Stress and strain distribution within the intact femur: compression or bending? *Med Eng Phys* 18:122–131
- Tilton FE, Degioanni TTC, Schneider VS (1980) Long term follow up on Skylab bone demineralisation. *Aviat Space Environ Med* 51:209–213
- Trinkaus E (1993) Femoral neck-shaft angles of the Qafzeh-Skhul early modern humans, and activity levels among immature Near Eastern Middle Paleolithic hominids. *J Hum Evol* 25: 393–416
- Trinkaus E, Ruff CB (1999) Diaphyseal cross-sectional geometry of Near Eastern Middle Palaeolithic humans: the femur. *J Archaeol Sci* 26:409–424
- Trinkaus E, Ruff CB, Conroy GC (1999) The anomalous archaic *Homo* femur from Berg Aukas, Namibia: A biomechanical assessment. *Am J Phys Anthropol* 110:379–391
- Wang Q, Strait DS, Dechow PC (2006) A comparison of cortical elastic properties in the craniofacial skeletons of three primate species and its relevance to the study of human evolution. *J Hum Evol* 51(4):375–382
- Weber GW, Bookstein FL (2011) *Virtual anthropology: a guide to a new interdisciplinary field*. Springer, New York
- Weber GW, Bookstein FL, Strait DS (2011) Virtual anthropology meets biomechanics. *J Biomech* 44(8):1429–1432
- Woo SL-Y (1981) The relationships of changes in stress levels on long bone remodeling, vol 45. American Society of Mechanical Engineers, Applied Mechanics Division, AMD, New York, pp 107–129
- Zienkiewicz O, Taylor R, Zhu J (2005) *The finite element method: its basis and fundamentals*. Elsevier, Oxford